Author/s:
Knarston, IM;Pachernegg, S;Robevska, G;Ghobrial, I;Er, PX;Georges, E;Takasato, M;Combes, AN;Jørgensen, A;Little, MH;Sinclair, AH;Ayers, KL

Title:
An In Vitro Differentiation Protocol for Human Embryonic Bipotential Gonad and Testis Cell Development

Date:
2020-12-08

Citation:
Knarston, I. M., Pachernegg, S., Robevska, G., Ghobrial, I., Er, P. X., Georges, E., Takasato, M., Combes, A. N., Jørgensen, A., Little, M. H., Sinclair, A. H. & Ayers, K. L. (2020). An In Vitro Differentiation Protocol for Human Embryonic Bipotential Gonad and Testis Cell Development. Stem Cell Reports, 15 (6), pp.1377-1391. https://doi.org/10.1016/j.stemcr.2020.10.009.

Persistent Link:
https://hdl.handle.net/11343/272278

Stem Cell Reports
Article
ISSCR
OPEN ACCESS

An *In Vitro* Differentiation Protocol for Human Embryonic Bipotential Gonad and Testis Cell Development

Ingrid M. Knarston,[1,2,7] Svenja Pachernegg,[1,2,7] Gorjana Robevska,[1] Irene Ghobrial,[1] Pei Xuan Er,[1] Elizabeth Georges,[1,2] Minoru Takasato,[3] Alexander N. Combes,[1,4] Anne Jørgensen,[5] Melissa H. Little,[1,2,6,8] Andrew H. Sinclair,[1,2,8] and Katie L. Ayers[1,2,8,*]

[1]Murdoch Children's Research Institute, Melbourne, Australia
[2]Department of Paediatrics, The University of Melbourne, Melbourne, Australia
[3]RIKEN Center for Biosystems Dynamics Research, Kobe, Japan
[4]Monash Biomedicine Discovery Institute, Department of Anatomy and Developmental Biology, Monash University, Melbourne, Australia
[5]Department of Growth and Reproduction, Copenhagen University Hospital, Copenhagen, Denmark
[6]Department of Anatomy and Neuroscience, The University of Melbourne, Melbourne, Australia
[7]These authors contributed equally
[8]Co-senior author
*Correspondence: katie.ayers@mcri.edu.au
https://doi.org/10.1016/j.stemcr.2020.10.009

SUMMARY

Currently an *in vitro* model that fully recapitulates the human embryonic gonad is lacking. Here we describe a fully defined feeder-free protocol to generate early testis-like cells with the ability to be cultured as an organoid, from human induced pluripotent stem cells. This stepwise approach uses small molecules to mimic embryonic development, with upregulation of bipotential gonad markers (*LHX9*, *EMX2*, *GATA4*, and *WT1*) at day 10 of culture, followed by induction of testis Sertoli cell markers (*SOX9*, *WT1*, and *AMH*) by day 15. Aggregation into 3D structures and extended culture on Transwell filters yielded organoids with defined tissue structures and distinct Sertoli cell marker expression. These studies provide insight into human gonadal development, suggesting that a population of precursor cells may originate from a more lateral region of the mesoderm. Our protocol represents a significant advance toward generating a much-needed human gonad organoid for studying disorders/differences of sex development.

INTRODUCTION

During mammalian embryonic development, the bipotential gonads develop on the ventromedial surface of the mesonephros and differentiate into either testes or ovaries based on the presence or absence of the Y sex chromosome. Disruption to gonadal development or function can result in disorders/differences of sex development (DSD) in humans, congenital conditions in which the anatomical, gonadal, or chromosomal sex is atypical (Hughes et al., 2006).

Currently only 40% of patients with a DSD receive a genetic diagnosis (Eggers et al., 2016), suggesting that unknown genes and genomic regions must contribute. When genomic sequencing identifies a novel DSD candidate gene variant, establishing pathogenicity is often hampered by a lack of appropriate human embryonic gonad cell lines. Thus, a reproducible human *in vitro* system comprising embryonic gonadal lineages is urgently required.

In recent years, directed differentiation of a wide range of cell lineages and tissues from human induced pluripotent stem cells (iPSCs) and embryonic stem cells (ESCs) has been achieved. Indeed, cardiac (Yang et al., 2008), intestinal (McCracken et al., 2011), cerebral (Lancaster and Knoblich 2014), and renal lineages (Takasato et al., 2014, 2015) have provided important disease models and an understanding of human embryonic development. Such an approach has the potential to provide an *in vitro* model of the human gonad. To date, several studies have used pluripotent cells to induce gonad-like cells: bipotential gonads (Sepponen et al., 2017), Sertoli or Leydig cells (Bucay et al., 2009; Buganim et al., 2012; Chen et al., 2019; Rodríguez Gutiérrez et al., 2018; Jadhav and Jameson 2011; Kjartansdóttir et al., 2015; Yang et al., 2015; Yang et al., 2017; Yazawa et al., 2006), and germ cell lineages (Hayashi et al., 2011; Irie et al., 2015; Hikabe et al., 2016; Shlush et al., 2017; Yamashiro et al., 2018; Gell et al., 2020). Some have overexpressed transcription factors to directly reprogram mouse or human fibroblasts into Sertoli and Leydig-like cells (Buganim et al., 2012; Jadhav and Jameson 2011; Yang et al., 2015, 2017; Yazawa et al., 2006). The ectopic expression of the transcription factors GATA4 and NR5A1 appears to be sufficient to reprogram human fibroblasts into Sertoli-like cells (Liang et al., 2019). Other protocols have used co-cultures of human and mouse cells (Rodríguez Gutiérrez et al., 2018; Shlush et al., 2017; Yamashiro et al., 2018) or co-cultures of human iPSCs with NT2D1 cells to differentiate Sertoli-like cells (Rodríguez Gutiérrez et al., 2018). Finally, bone morphogenetic protein (BMP) and WNT signaling drives bipotential gonad marker expression in human ESCs without the requirement for co-culture or transfection/transduction (Sepponen et al., 2017). Despite these advances, differentiation

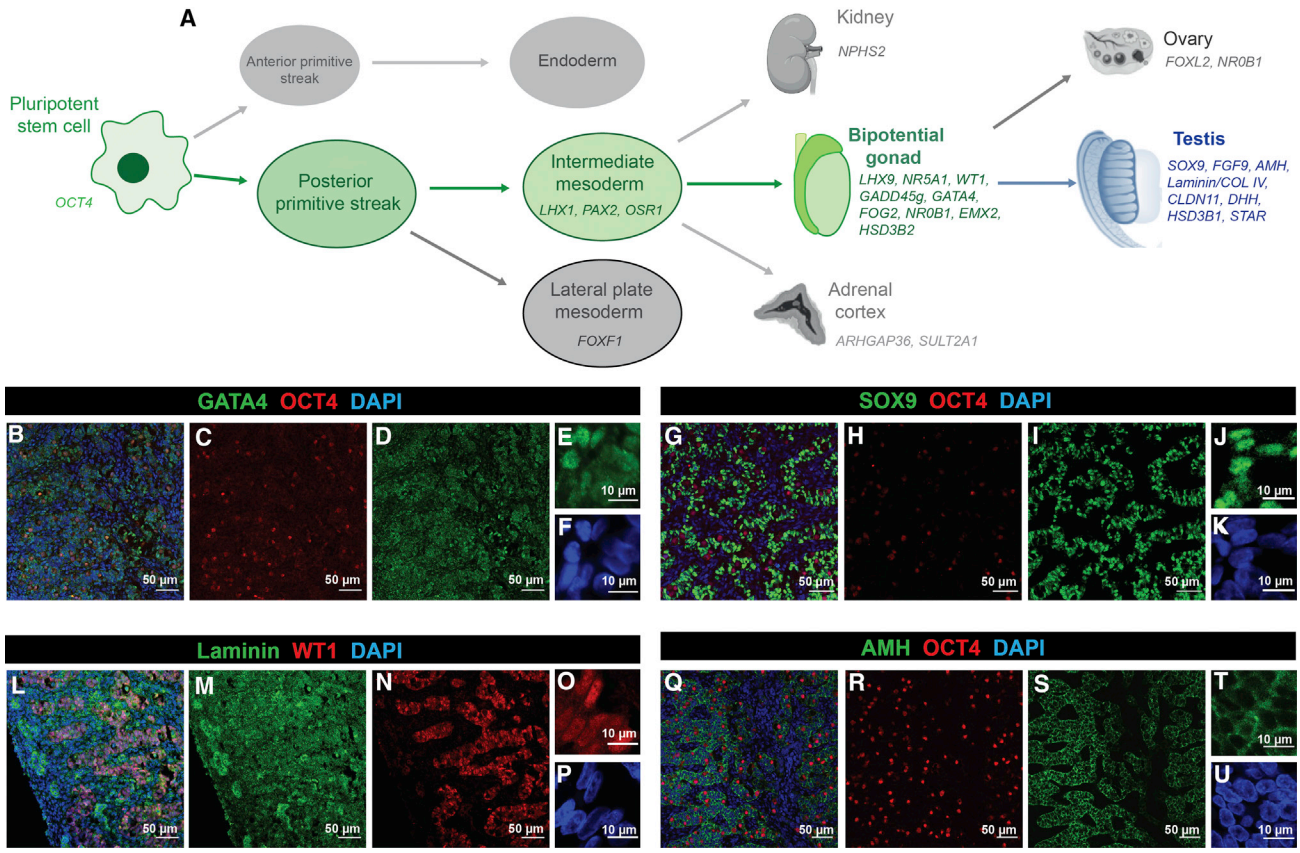

Figure 1. Stepwise Gonadal Differentiation and Expression of Markers in Human Fetal Testes

(A) Schematic of directed differentiation of human iPSCs through the posterior primitive streak, intermediate mesoderm, and bipotential gonad to the testes. Genetic markers are shown.

(B–U) Human fetal testes sections (week 9 gestation) stained for Sertoli cell markers: GATA4 (B, D, and E, green), SOX9 (G, I, and J, green), WT1 (L, N, and O, red), and AMH (Q, S, and T, green). Germ cells are marked with OCT4 (B, C, G, H, Q, and R, red). Basement membrane is stained with Laminin (L and M, green). DAPI stains cell nuclei (B, F, G, K, L, P, Q, and U, blue). B, G, L, and Q are overlays and E, F, J, K, O, P, T, and U are high magnification.

of control or patient iPSCs into a stable population that accurately recapitulates the early human embryonic gonad without the need for co-culture or lentiviral induction remains elusive. Furthermore, culturing of these differentiated cells in a three-dimensional (3D) organoid to model the complex cellular structures and interactions of the embryonic gonad has not yet been demonstrated.

This study aimed to generate testis lineages from human iPSCs. Specifically, we employed a stepwise directed differentiation approach to guide cells through developmental cell populations that ultimately give rise to the bipotential gonads and early Sertoli cells. We present a novel feeder-free protocol for the induction of these lineages from human iPSCs in approximately 15 days. Furthermore, culturing of these cells in 3D led to the development of defined tissue structures with distinct expression of Sertoli cell markers. This work has given us insight into the potential origin and regulatory interactions during human gonad development. It represents a significant step toward a human iPSC-derived *in vitro* model for embryonic gonad/testis development and DSD.

RESULTS

Identification and Characterization of Appropriate Markers of the Human Embryonic Bipotential Gonad and Early Testis

During embryonic development, the posterior primitive streak (PS) gives rise to the intermediate mesoderm (IM). In mice, the coelomic epithelium overlaying the IM develops into the somatic cells of the bipotential gonad (Karl and Capel 1998) (Figure 1A). To characterize cell identity during differentiation of human iPSCs to gonadal cells,

we devised a panel of marker genes for gonad development (Figure 1 and Table S1). Publicly available RNA-sequencing (RNA-seq) data from mouse, including bulk RNA-seq from embryonic day (E) 10.5–E13.5 gonads (Zhao et al., 2018) and single-cell RNA-seq (scRNA-seq) of sorted gonadal cells (Stévant et al., 2019), were interrogated to confirm marker expression. The *Lhx9*, *Nr5A1*, *Gadd45g*, *Wt1*, *Gata4*, *Fog2/Zfpm2*, *Nr0B1*, *Emx2*, and *Hsd3b2* genes were chosen to represent the bipotential gonad. These are expressed in mouse embryonic gonads between E10.5 and E11.5 and then decrease as the gonads differentiate. Of these, *Lhx9*, *Wt1*, *Gata4*, and *Emx2* have the earliest expression, in the early pre-Sertoli and pre-granulosa cells. Expression was also assessed in human fetal gonad datasets, including an RNA-seq dataset from 7–19 weeks gestation (Guo et al., 2015) and scRNA-seq data (weeks 4–26 gestation ovaries and testis) (Li et al., 2017). Analysis using the ReproGenomics Viewer (Darde et al, 2015, 2019) confirmed early expression of these bipotential gonad markers, with the caveat that in humans, *LHX9*, *WT1*, and *EMX2* are expressed more strongly in the early female tissues (Figures S1A–S1C). These data confirmed the expected specificity of our bipotential gonad markers to the somatic cells, with the exception of *GATA4*, which also has some low-level expression in the primordial germ cells (Figure S1F).

For testis, we chose *SOX9*, *FGF9*, *AMH*, *CLAUDIN11* (*CLDN11*), and *DHH* as Sertoli cell markers. *Sox9* and *Fgf9* are among the earliest markers of testis development, along with *Sry*, in the mouse gonad (peaking at E11.5) and in humans (peaking at 7–7.5 weeks gestation) (Belle et al., 2017). In mouse gonads, *Sox9* activates the *Amh* gene at E12. In mouse, *Amh* expression is also observed in granulosa and endothelial cells, whereas in humans it appears more specific to the Sertoli cells, as does the mature Sertoli cell marker *CLDN11* (Figures S1E and S1J).

Expression of the Leydig markers *Star* and *Hsd3b1* peaks at later time points in mouse, as Leydig cells differentiate in response to Sertoli cell signaling. In the mouse, these markers are highly specific to testis, with little expression in ovary. In human, *STAR* appears to be expressed in both testis and ovarian cells (Figure S1G), and *HSD3B1* shows almost no expression in human gonads (Figure S1H). *GATA4* and *NR5A1* also show Leydig expression in humans (Figures S1F and S1I).

To address gonadal specificity, marker gene expression was evaluated in the IM-derived kidney and adrenal cortex. Expression datasets for human fetal kidney (Lindström et al., 2018), human iPSC-derived kidney organoids (Phipson et al., 2019; Takasato et al., 2015), and embryonic mouse kidney (Combes et al., 2019) (Figures S1O–S1Q) revealed that several markers exhibited widespread expression, such as *EMX2* and *WT1*, whereas *GATA4*, *AMH*, *LHX9*, and *NR5A1* show greater gonad specificity. A microarray study on human fetal adrenal gland, kidney, and gonads (Del Valle et al., 2017) indicated that *NR5A1*, *NR0B1*, *HSD3B2*, and *STAR* are also expressed in developing adrenal lineages (Figures S1K–S1N).

Markers to screen for unwanted cell types, i.e., precursor populations (pluripotent stem cells, *OCT4*; IM cells, *LHX1*, *PAX2*, *OSR1*; lateral plate mesoderm [LPM], *FOXF1*), non-gonadal IM-derived tissues (adrenal, *ARHGAP36*, *SULT2A1*; kidney, *NPHS2*), and ovarian cells (*FOXL2* and *NR0B1*), were also included (Figure 1A and Table S1).

Several gonadal markers were validated using immunofluorescence (IF) staining of week 9 human fetal testes, some of which have not been previously reported (Figures 1B–1U). GATA4 had the highest expression in the testis cords, where it showed strong nuclear staining with some weak staining or background outside of the cords. This protein also appeared to have low-level cytoplasmic staining (Figures 1B, 1D, and 1E). The Sertoli cell markers SOX9 (Figures 1G, 1I, and 1J), WT1 (Figures 1L, 1N, and 1O), and AMH (Figures 1Q, 1S, and 1T) had testis cord-specific staining. SOX9 is strongly nuclear with some weak cytoplasmic staining (Figure 1J), while WT1 is nuclear (Figure 1O) and AMH is mostly cytoplasmic (Figure 1T). OCT4 is nuclear in germ cells (Figures 1B, 1C, 1G, 1H, 1Q, and 1R). Laminin marked epithelial basement membrane throughout the testis, with strong expression surrounding the cords—best visualized at the edge of the gonadal section (Figures 1L and 1M).

Delineating the Origins of the Human Embryonic Gonad

In humans, the bipotential gonad is widely considered to arise from the IM between weeks 5 and 6 of embryonic development (Satoh 1991). The trunk mesoderm, including the IM, forms from cells arising from the posterior PS as the body axis elongates (Figure 2A) (Takasato and Little 2015), giving rise to a host of different tissues depending upon the positioning of these cells along the streak at the time of exit. As the trunk elongates, differentiation into distinct regions of organ primordia is specified by gradients of morphogenic factors signaling along the various axes, including craniocaudal, dorsoventral, and mediolateral. Hence, the patterning to gonad requires precise control of fate initially with respect to position within the PS and the axes of the body plan.

As both the mammalian kidney and the gonad arise from the IM (Karl and Capel 1998), we used a renal differentiation protocol (Takasato et al., 2015) as a starting point to create gonadal cells *in vitro*. This stepwise differentiation guides iPSCs through the posterior PS using the GSKβ inhibitor/WNT signaling activator, CHIR99021 (CHIR). The WNT signaling pathway patterns the anterior-posterior axis of the PS (Figure 2A),

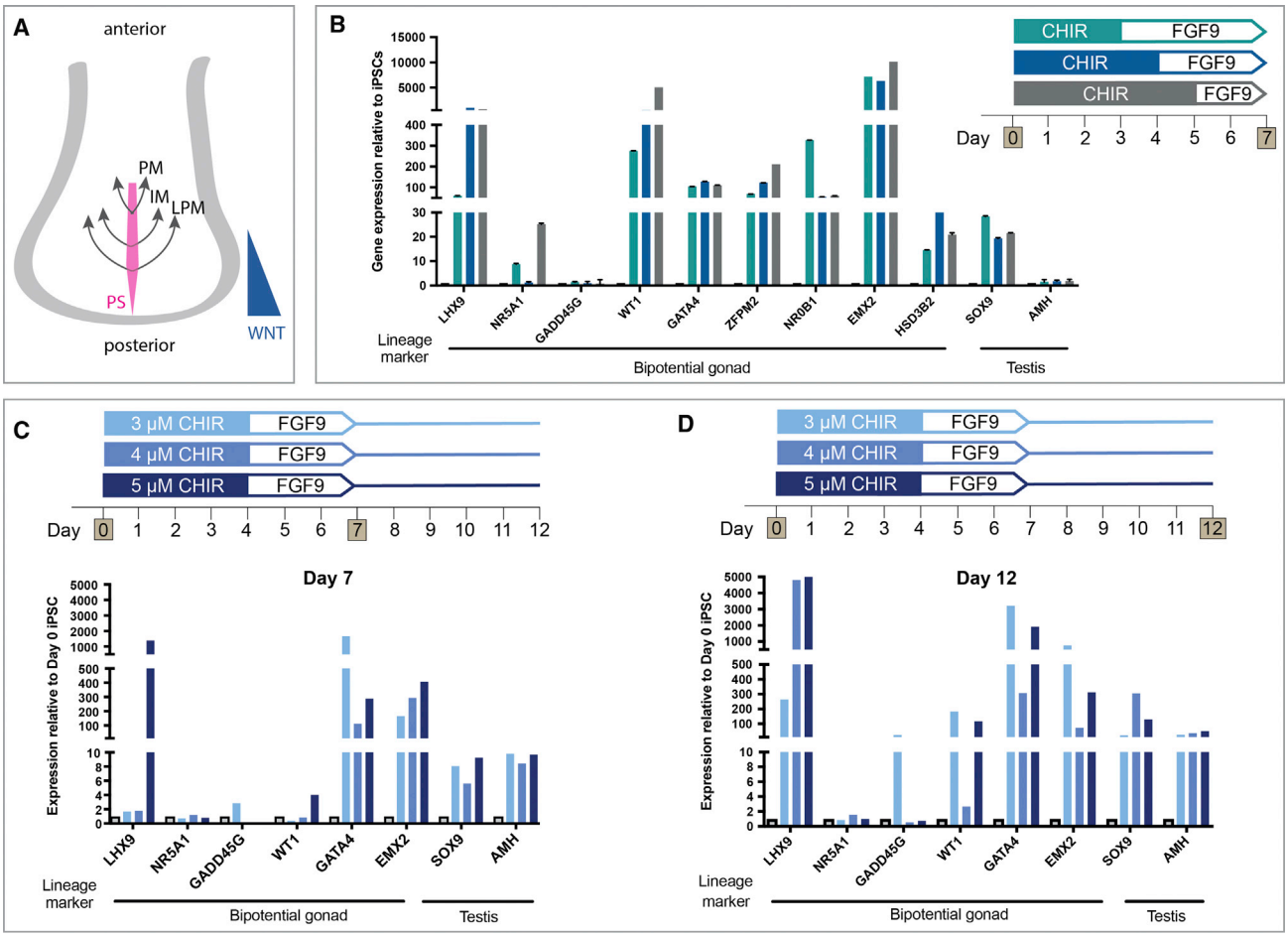

Figure 2. Testing the Induction of Gonad Lineages Along the Anterior-Posterior Axis

(A) The paraxial mesoderm (PM), intermediate mesoderm (IM), and lateral plate mesoderm (LPM) arise from the posterior primitive streak (PS), which is patterned anterior-posteriorly by WNT signaling.

(B) Relative gene expression (qRT-PCR) of bipotential gonad and testis markers after 7 days of differentiation with 3, 4, or 5 days of 4 μM CHIR treatment. Each sample represents three independent differentiations (biological replicates) with three technical replicates (mean ± SEM).

(C and D) Differentiation with 3, 4, or 5 μM CHIR for 4 days followed by 3 days FGF9. Relative gene expression of gonad markers after (C) 7 and (D) 12 days of differentiation. Each sample represents three technical replicates of one differentiation (mean ± SEM). Gene expression is quantified relative to day 0 iPSCs.

which can be altered by changing CHIR concentration or duration (Takasato et al., 2015). To form kidney organoids, the differentiating cultures were guided toward an IM lineage (*OSR1/LHX1/PAX2*$^{+}$) with FGF9 (Takasato et al., 2015), although changes in the initial CHIR duration also appeared to shift between more cranial (anterior IM) and caudal (posterior IM) identities (Takasato et al., 2015). We aimed to identify the optimal conditions under which gonadal precursor cells (GPCs) would arise using a male control iPSC line. The kidney protocol used 8 μM CHIR (Takasato et al., 2015), but as a lower CHIR concentration has previously been shown to induce gonadal differentiation of human ESCs (Sepponen et al., 2017), we started by using 4 μM CHIR with varied duration (3, 4, or 5 days with 4 μM CHIR followed by 200 ng/mL FGF9). Bipotential gonad and testis marker expression was assessed in differentiated cells relative to day 0 iPSCs (Figure 2B). After 7 days, the bipotential gonad markers *LHX9*, *WT1*, *GATA4*, *ZFPM2*, *NR0B1*, *EMX2*, and *HSD3B2* were induced under all three conditions. Low-level induction of the early Sertoli marker *SOX9* was also observed (Figure 2B). For many of these markers, expression was similar between CHIR

durations, with the exception of *LHX9*, *WT1*, and *HSD3B2*, for which a longer CHIR treatment induced higher expression, and *NR0B1*, for which a shorter duration induced higher expression (Figure 2B). *NR5A1* showed generally low expression, with significant induction seen only with CHIR treatment for 5 days. Notably, *GADD45g* was also expressed in the day 0 iPSCs, and its expression did not increase after 7 days under any condition. *AMH* was not upregulated under any condition, indicating that additional factors may be necessary to induce Sertoli cell maturation. Given these results, an intermediate duration (4 days) of CHIR was used subsequently.

Next, CHIR concentration was tested (3, 4, or 5 μM) with markers assessed at day 7 (Figure 2C) and day 12 (Figure 2D). At day 7, the bipotential gonad markers *LHX9*, *GATA4*, and *EMX2* were highly induced and *GADD45g* and *WT1* were induced at lower levels (Figure 2C). Of these markers, *LHX9*, *EMX2*, and *WT1* responded best to 5 μM CHIR, whereas *GATA4* and *GADD45g* responded best to 3 μM (Figure 2C). After 12 days of differentiation, continued induction of the bipotential gonad markers was observed, with significant induction of *LHX9* under all three conditions (Figure 2D). *GADD45g*, *WT1*, *GATA4*, and *EMX2* responded best to 3 μM CHIR. By day 12, evidence for the activation of the testis pathway (Sertoli cell markers) was also observed, with a 50- to 300-fold induction of *SOX9* and a 20- to 50-fold increase in *AMH* expression relative to the day 0 control (Figure 2D). Hence, 3 μM CHIR for 4 days is optimal for gonadal/testis marker induction.

Along the mediolateral axis, the mesoderm forms paraxial mesoderm, IM, and LPM from the center to the periphery, respectively (Figure 3A). Although often described as discrete regions, these likely represent a continuum patterned by growth factor gradients both mediolaterally and dorsoventrally. The best characterized of the mediolateral patterning factors is BMP4. BMP4 is produced within the LPM, and BMP pathway activity is higher in the more lateral tissue (Figure 3A). Takasato et al. (2015) found that the addition of FGF9 from day 4 induced IM, which was optimal without the addition of exogenous BMP4 or inhibition of this pathway. Whereas mouse studies have suggested an IM origin for the gonad (Karl and Capel 1998), lineage tracing in the chicken found that GPCs arise from the LPM (Yoshino et al., 2016). Indeed, BMPs can induce bipotential gonad markers in human ESCs (Sepponen et al., 2017). To investigate if slight lateralization using BMP4 improves induction of a GPC fate, two different concentrations of BMP4 were tested (5 and 50 ng/mL) together with FGF9. Gene expression was assessed after 7 days (Figure 3B). A decline in the IM marker *LHX1* and increased expression of the LPM marker *FOXF1* indicated that BMP4 was shifting cell identity laterally (Figure 3B). Some bipotential gonad markers (*LHX9*, *ZFPM2*, *AMH*) responded equally with the varying BMP4 concentrations. Others (*WT1*, *NR5A1*, *EMX2)* were best induced with no or low-level BMP4 and seemed to be inhibited by high levels of BMP4. *GADD45g*, *GATA4*, *NR0B1*, *HSD3B2*, and *SOX9* were upregulated with increased concentrations of BMP4 (Figure 3B). As most markers were expressed under all conditions, while a high concentration of BMP4 inhibited the expression of two essential bipotential gonad genes (*WT1*, *EMX2*), we chose an intermediate BMP4 concentration (10 ng/mL) for further experiments. The robustness of these results (CHIR duration/concentration and BMP4) was confirmed in an independent, female, iPSC line, CRL1502.3 (Figures S2A–S2C). In conclusion, bipotential gonad and testis markers are activated with a shortened and lower concentration of initial CHIR induction followed by addition of FGF9 and intermediate BMP4 levels.

Gonadal Cell Induction and Testis Differentiation Are Enhanced by Extended Culture with Prostaglandin D2

We tested several growth factors for their ability to induce testis gene expression. In mice, prostaglandin D2 (PGD_2) is involved in a feedback loop to upregulate *SOX9* in testis (Wilhelm et al., 2005). We differentiated cells with or without 500 ng/mL PGD_2 from day 10 to 18 to optimize testis cell induction after initial *SOX9* expression. At day 18, *SOX9* and *AMH* were higher with PGD_2 (Figure 3C), while substantial *SOX9* staining was observed after 18 days (Figure 3D). Some 3βHSD was also observed (Figure 3D). This suggests that prolonged culture and PGD_2 treatment leads to improved testis lineage induction. Previous studies have shown that inhibition of Hedgehog signaling blocks gonadal development (Yoshino et al., 2016), while retinoic acid (RA) signaling is important in mesodermal segmentation (Duester 2008) and mouse gonad outgrowth (Sandell et al., 2007). Hence, cultures were treated with either a Hedgehog signaling agonist (SAG) or RA from day 4 to 7 of differentiation. After 7 days, a dose-dependent reduction in the markers *WT1*, *ZFPM2*, *NR0B1*, *EMX2*, and *HSD3B2* was observed after SAG treatment (Figure S2D), and expression of *NR5A1*, *EMX2*, *AMH*, and *SOX9* was reduced following RA treatment (Figure S2E). Hence, SAG and RA were excluded from further differentiations.

An Optimized Differentiation Protocol for Human Bipotential Gonad and Testis Cells

The above studies provided an optimized protocol for bipotential gonad and Sertoli-like cell differentiation in monolayer cultures (Figure 4A). To confirm our protocol,

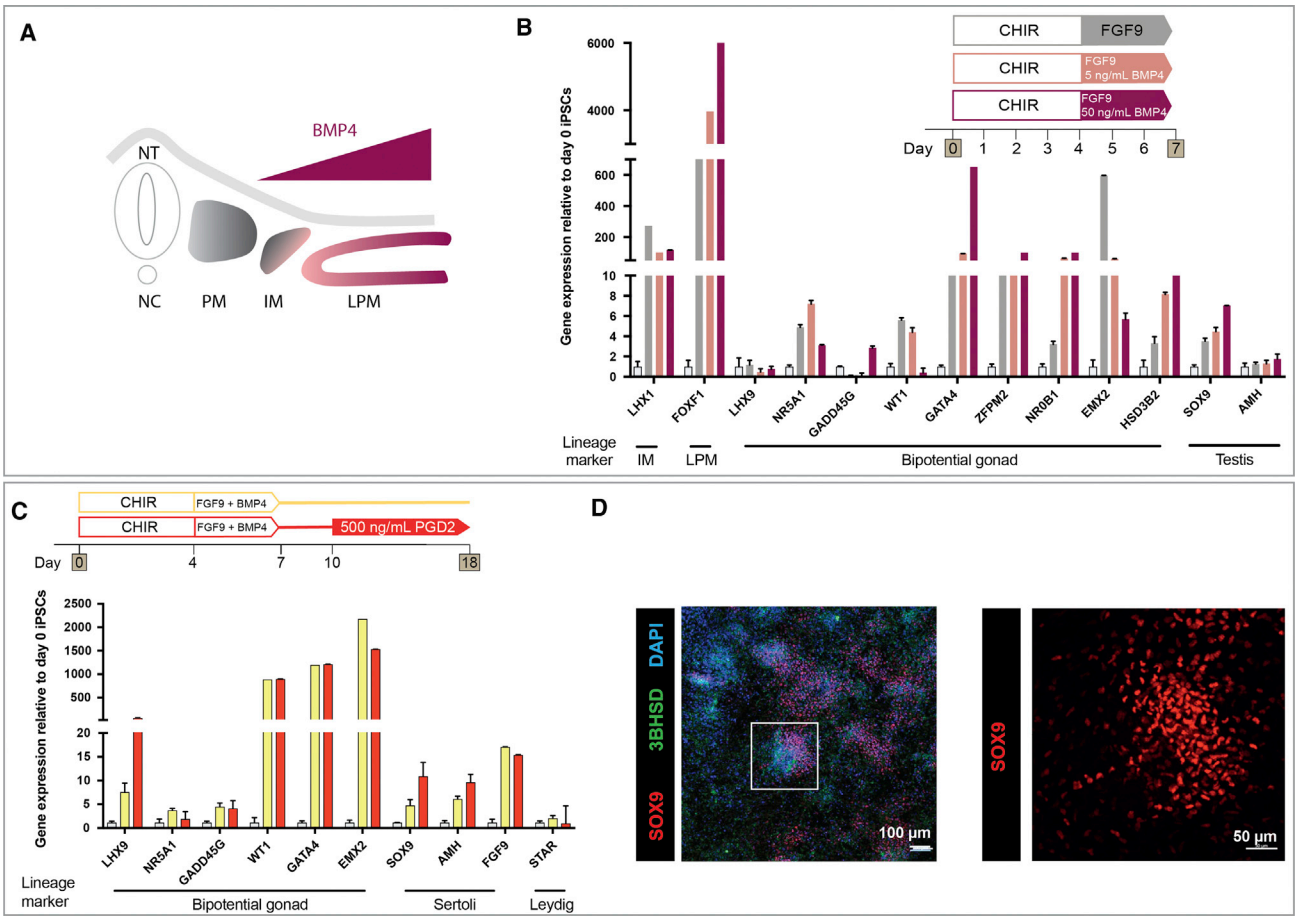

Figure 3. Shifting Differentiation toward the Lateral Plate Mesoderm Favors Induction of Some Gonadal Markers, and PGD_2 Induces Testis-like Cell Differentiation

(A) The BMP4 gradient patterns the mesoderm along the mediolateral axis. Higher BMP4 concentrations shift fate laterally. IM, intermediate mesoderm; LPM, lateral plate mesoderm; NC, notochord; NT, neural tube; PM, paraxial mesoderm.

(B) qRT-PCR showing relative gene expression of markers after 7 days of differentiation with 0, 5, or 50 ng/mL BMP4 treatment following CHIR99021 (CHIR). Each sample represents three technical replicates of one differentiation (mean ± SEM).

(C) Relative gene expression of bipotential gonad and testis markers after 18 days of differentiation with or without 500 ng/mL PGD_2 from day 10 to 18. Each sample represents four independent differentiations with three technical replicates (mean ± SEM). Gene expression is quantified relative to day 0 iPSCs.

(D) IF staining of day 18 monolayer culture with 500 ng/mL PGD_2 addition. Staining was for the Sertoli cell marker SOX9 (red) and Leydig cell marker 3βHSD (green). DAPI (blue) stains cell nuclei.

it was replicated in two independent iPSC lines (PCS_201_010 iPC clone 5 cells, n = 4, and CRL1502.3 clone 32 cells, n = 5) (Figures 4B–4F; see also S5). The pluripotency marker *OCT4* was most expressed in day 0 iPSCs and significantly decreased thereafter, while IM (*LHX1*, *PAX2*) and LPM markers (*FOXF1*) peaked at day 7 (Figure 4B). At this time, early bipotential gonad markers (*GATA4*, *ZFPM2*, *EMX2*, *NR0B1*) were induced (Figure 4C), with remaining bipotential gonad markers induced between days 7 and 10 (*LHX9*, *NR5A1*, *GADD45g*, *WT1*). These often continued to be expressed until day 15, albeit at lower levels. The expression of these markers mimics what is seen in mouse bipotential/E10.5 gonads. Most Sertoli cell markers become induced by day 10, although *FGF9* peaks at day 7, perhaps in response to the addition of FGF9 to the medium (Figure 4D). This may kick-start *SOX9* expression, which in turn activates *AMH* expression. *CLDN11*, initially expressed at day 7, has increased expression at day 15 (Figure 4D). Sertoli markers were analyzed by IF (Figures 5, see also S3 and S4). Similar to qPCR findings, GATA4 was weakly expressed at day 7 (Figures 5B and

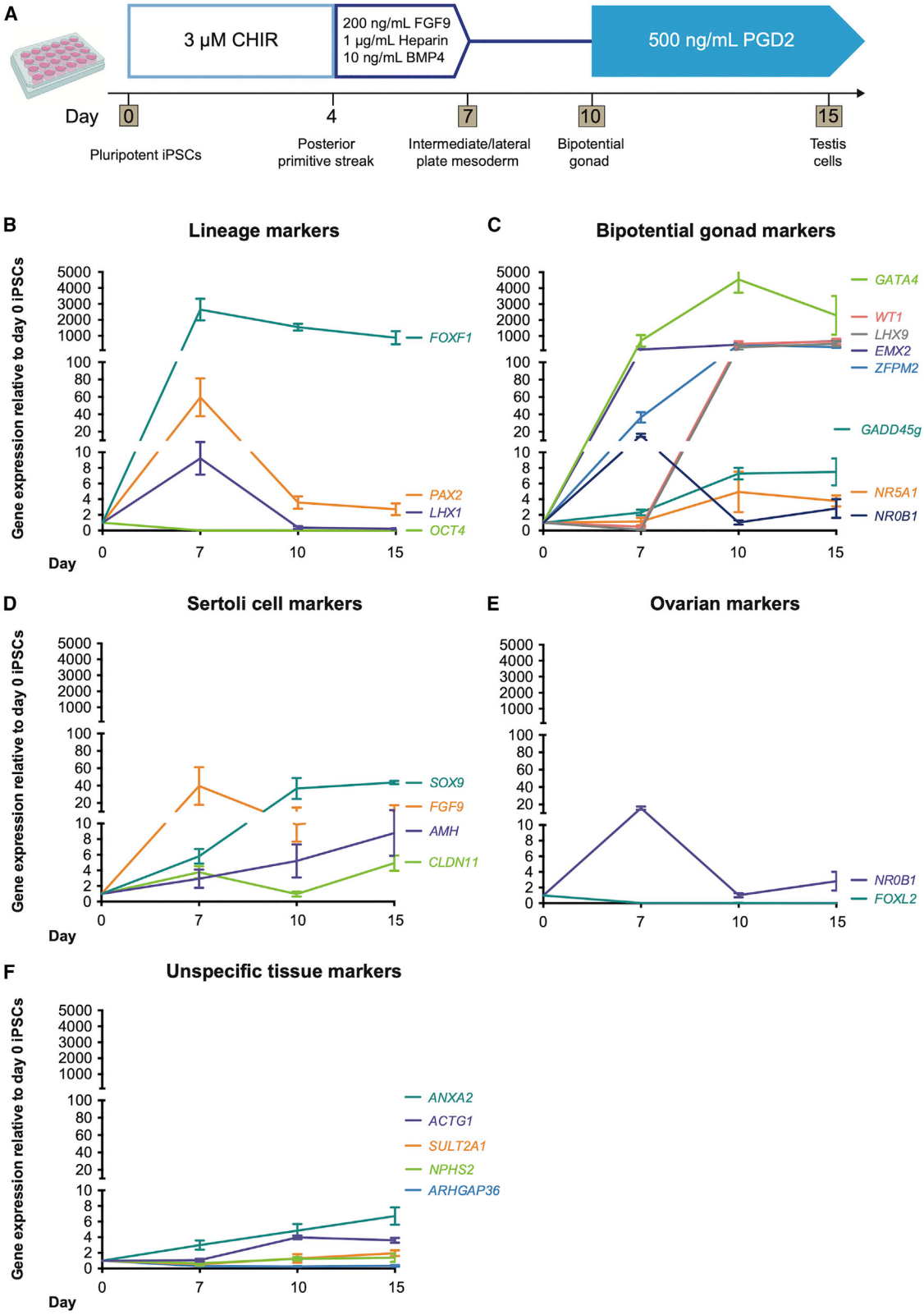

(legend on next page)

5F), and this expression increased over time (Figures 5J, 5N, 5R, 5V, S3Q–S3T, and S4K–S4T). Quantification to account for different cell numbers indicated that the mean GATA4 expression levels increase in each cell over time (Figure S4S). Like GATA4, SOX9 expression is weak at day 7 (Figures 5C and 5G) and increases over time, with SOX9 becoming localized to specific cellular groups (Figures 5K, 5O, 5S, 5W, S3A–S3D, and S4A–S4J). Quantification of SOX9 levels per cell (including in day 0 controls) indicated that expression increases only in a subset of cells, with other cells expressing a baseline level that does not appear to increase (Figures S4I and S4J). Sertoli markers WT1, CLDN11, and AMH showed increased expression after day 7, with AMH and CLDN11 showing significant expression by day 15 (Figures S3I–S3P, S3W, and S3X). WT1 protein appears to decrease or become more restricted from day 10, although RNA levels stay the same (Figures 4C and S3E–S3H). Cultures were also extended to 21 days (Figures 5Q–5X). At this stage, high expression of both GATA4 and SOX9 becomes restricted to cell clusters, which become elongated compared with day 15 clusters (Figures 5R, 5V, 5S, and 5W). Basement membrane proteins (Laminin or Collagen IV) were expressed in both day 15 and day 21 differentiated cells and surrounded the GATA4/SOX9-positive cell clusters (Figures 5L, 5P, 5T, and 5X). A similar induction in Sertoli cell proteins was observed in the CRL1502.3 clone 32 line, although this appeared to be reduced after day 15 in this line (Figures S3A′–S3Y′).

The Leydig cell marker *STAR* was upregulated 4-fold at day 10 with some IF staining at all time points (Figures S5B–S5E). A second Leydig marker, *HSD3B1*, was upregulated at the RNA level (Figure S5A), and 3βHSD staining was observed in some cells (Figure 3D). Finally, the female gene *FOXL2* was not expressed, while *NR0B1* was expressed at day 7 and then downregulated (Figure 4E). These results indicate the formation of bipotential gonads and testis cells, including Sertoli-like and possibly Leydig-like populations.

Although most of our markers suggest that we are creating a gonadal cell lineage, expression of *SOX9* and *WT1* could also signal the differentiation of chondrocytes or kidney cells. We found that the kidney marker *NPHS2* was not significantly induced, nor were the adrenal markers *ARHGAP36* or *SULT2A1* (Figure 4F). Two chondrocyte progenitor markers, *ACTG1* and *ANXA2*, also showed only low-level induction (4- to 6-fold) (Figure 4F).

Similar results for all of the above markers were obtained using a second, independent iPSC line (Figures S5G–S5K). We conclude that our 15-day differentiation protocol specifically and robustly guides iPSCs through the IM into the bipotential gonad and then to a Sertoli-like cell fate.

Human iPSC-Derived Bipotential Gonad Cells Show Self-Organizing Abilities

Previous studies have shown that dissociated and reaggregated mouse urogenital ridges have the capacity to form testicular structures maintaining expression of important testis/germ cell markers (McLaren and Southee 1997; Bowles et al., 2006). This ability decreases with developmental age (Escalante-Alcalde and Merchant-Larios, 1992) (Figure S6). We confirmed that at E12.5 testis cells were better able to reassociate into structures in which $SOX9^+$ cells surround E-cadherin$^+$ germ cells (Figures S6D and S6H). At E13.5, these structures are still formed upon reaggregation, while at E14.5, these structures fail to form with germ cells located at the periphery (Figures S6F–S6K). This suggests that to create a 3D organoid model of the human testis, cellular aggregates should be generated when patterning has reached bipotential gonad or early differentiated testis. We therefore investigated whether the iPSC-derived bipotential gonad cells were able to self-organize into 3D structures similar to mouse gonad reaggregation. Our optimized monolayer differentiation protocol (Figure 6A) was used to differentiate monolayer cells. At day 7, differentiated cells were pelleted as described previously (Takasato et al., 2015) and cultured on Transwell filters for a further 14 days, maintaining PGD_2 treatment from day 10 to 21 (Figure 6A). At day 21, the organoids were approximately 2–3 mm wide with undefined tissue surrounding a thicker center containing round and tubular-like structures (Figure 6B). The lineage markers *FOXF1*, *OSR1*, *PAX2*, and *LHX1* peaked at day 7 and decreased after (Figure 6C). A lower expression of *LHX1* with a higher expression of the LPM marker *FOXF1* in organoids may indicate a shift

Figure 4. A Protocol for the Stepwise Induction of Testis-like Cells from Human iPSCs

(A) The optimized monolayer differentiation protocol. Cells are cultured for 4 days with 3 μM CHIR; 3 days with 200 ng/mL FGF9, 1 μg/mL heparin, and 10 ng/mL BMP4; 3 days without growth factors; and then 500 ng/mL PGD_2 from day 10. RNA is harvested at days 0, 7, 10, and 15.

(B–F) qRT-PCR data of relative gene expression after 7, 10, and 15 days of monolayer differentiation for (B) lineage markers (*OCT4*, pluripotency; *FOXF1*, LPM; *LHX1/PAX2*, IM), (C) bipotential gonad markers, (D) Sertoli cells, (E) ovarian differentiation, and (F) non-target tissues (*ANXA2/ACTG1*, chondrocyte progenitors; *ARHGAP36/SULT2A1*, embryonic adrenal; *NPHS2*, embryonic kidney). Each sample represents four independent differentiations with three technical replicates each (mean ± SEM). Gene expression is quantified relative to day 0 iPSCs.

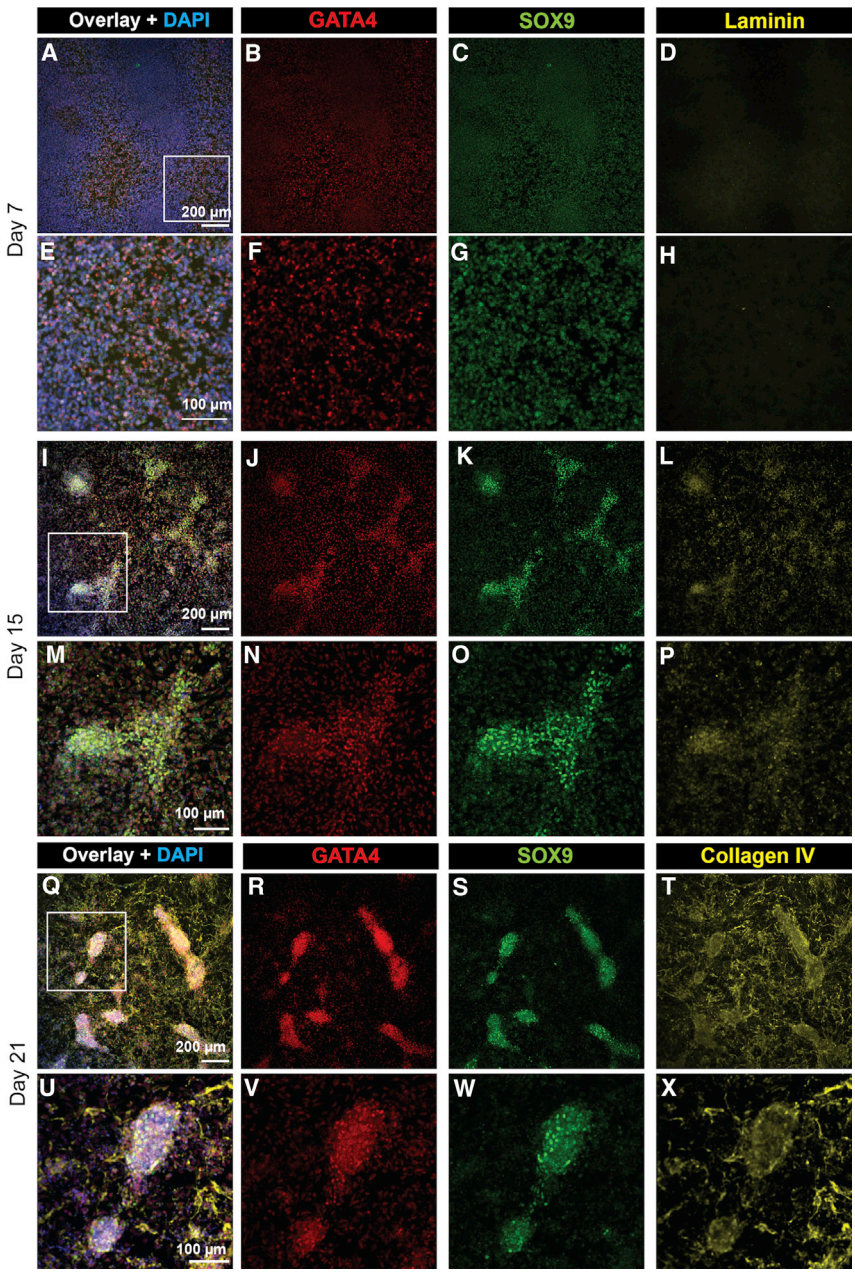

Figure 5. Gonadal Markers Are Upregulated at the Protein Level Following Human iPSC Differentiation

(A–H) IF staining at day 7, (I–P) day 15, and (Q–X) day 21 of differentiation. (B and F) GATA4 expression is evident from day 7, with a subset of cells showing a high level of staining that increases over time (B, F, J, N, R, and V). (C and G) SOX9 expression is present in low levels at day 7 and increases strongly in intensity by (K and O) day 15 and (S and W) day 21 in a subset of cells that partially overlap those showing high GATA4 expression (C, G, K, O, S, and W). (Q–X) On day 21 of differentiation, elongated $SOX9^{+-}$ $GATA4^{+}$ clusters can be observed. (D, H, L, and P) Laminin or (T and X) Collagen IV marks basement membrane. (A, E, I, M, Q, and U) Overlays with DAPI (blue). (E–H, M–P, and U–X) Higher magnification images of the boxed regions in (A, I, and Q), respectively.

toward a more lateral fate (Figure 6C). Bipotential gonad markers (*EMX2*, *WT1*, *LHX9*, *GATA4*) were highly expressed in day 21 organoids (Figure 6D) and, while not consistently observed in the monolayer, *NR5A1* was induced in the organoids (12- to 15-fold). The Sertoli cell markers *SOX9*, *AMH*, and *CLDN11* also showed induction between days 7 and 21 (Figure 6E). *SOX9* in particular was expressed at higher levels in day 21 organoids than in the day 15 monolayer cultures (100- to 120-fold in organoids; 45-fold in monolayer). *DHH* expression was also observed in the day 21 organoids (Figure 6E). The Leydig cell markers *CYP11A1*, *CYP17A1*, *HSD3B*, and *STAR* were all upregulated in day 21 organoids, comparable to what we observed in monolayer cultures of the same age (Figure S6).

We carried out IF staining of day 21 organoids (Figure 6, see also S6). IF showed SOX9 (Figures 6F, 6G, 6J, and 6K) and GATA4 (Figures 6F, 6H, 6J, and 6L) protein expression. Like day 15 and day 21 monolayer cultures, clusters of cells had strong SOX9 expression in particular on the periphery and within the tubular structures (Figures 6G and 6K). SOX9 staining partially overlapped with GATA4, which appeared more widespread (Figures 6H and 6L). The basement membrane marker Laminin was

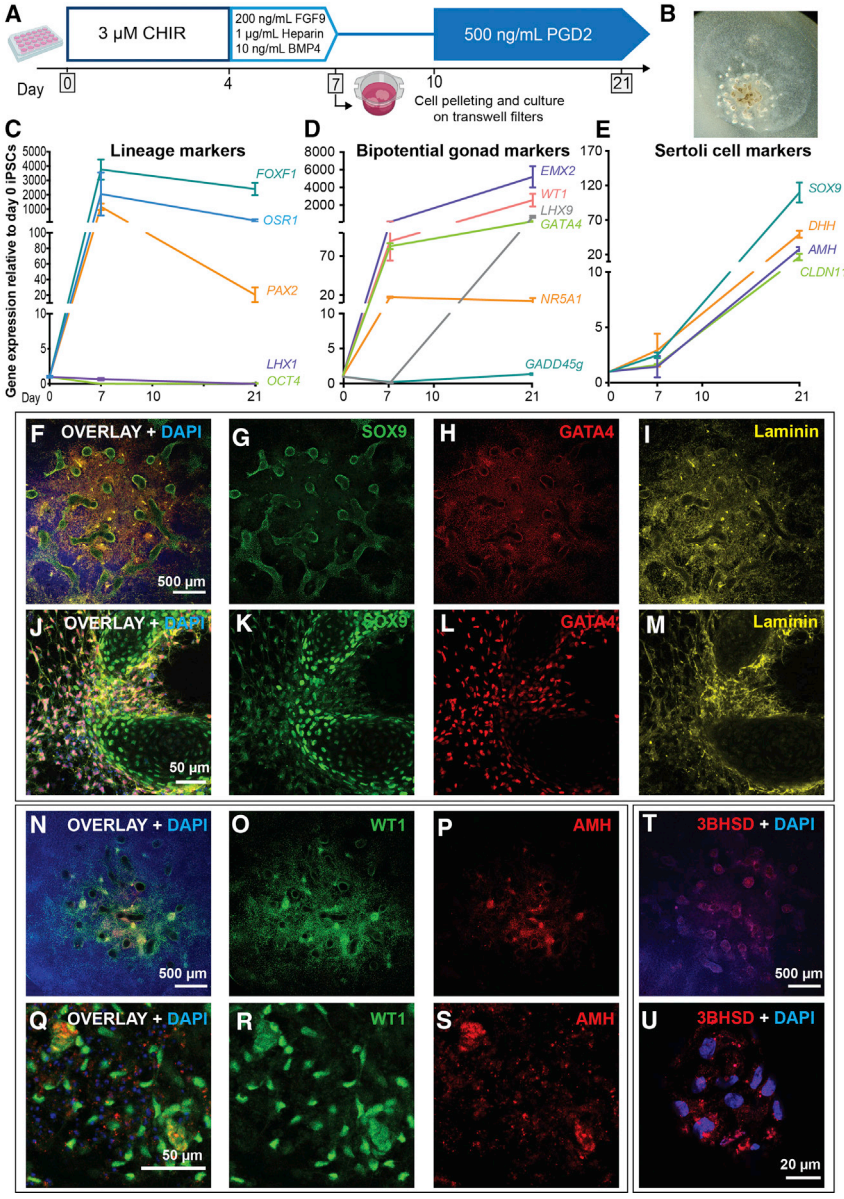

Figure 6. Bipotential Gonad and Sertoli Cell Markers Are Upregulated in Gonadal Organoids

(A) Optimized protocol with day 7 cells pelleted and cultured on Transwell filters.

(B) Day 21 organoids are approximately 3 mm wide and flat, showing defined structures in the thicker center.

(C–E) Relative gene expression of (C) lineage markers (*OCT4*, pluripotency; *FOXF1*, LPM; *LHX1/PAX2/OSR1*, IM), (D) bipotential gonad markers, and (E) Sertoli cell markers in day 0 and day 7 cells and day 21 organoids. Each sample represents three independent differentiations with three technical replicates (mean ± SEM). Gene expression is quantified relative to day 0 iPSCs.

(F–U) IF of organoids shows that SOX9 (F, G, J, and K, green) and GATA4 (F, H, J, and L, red) are strong in specific cell clusters, also marked by Laminin (F, I, J, and M, yellow). (J–M) Magnification of part of (F–I). WT1 (N, O, Q, and R, green) and AMH (N, P, Q, and S, red) staining is also present in a subset of cells. (Q and R) Magnified view. (T and U) 3βHSD staining in a subset of cells. (F, J, N, and Q) are overlay images with DAPI which stains nuclei (blue).

present throughout the organoids, often with expression higher in cells on the periphery of the tubular structures (Figures 6I and 6M). WT1 had strong expression in a subset of cells, similar to SOX9 (Figures 6N, 6O, 6Q, and 6R), some of which also appeared to have AMH staining (Figures 6P and 6S). These cells also showed Collagen IV staining (Figures S6L–S6O). An antibody for 3βHSD indicated punctate cytoplasmic staining in a subset of cells associated with the tubular structures (Figures S6T and S6U), and the Leydig marker STAR also stained a small subset of cells (Figures S6T and S6U). The apoptosis marker cleaved Caspase 9 showed a small amount of scattered cell death, but no widespread apoptosis (Figures S6P and S6Q).

In summary, human iPSC-derived bipotential gonad cells show the ability to self-organize into 3D gonadal structures with significant expression of testis cell markers.

DISCUSSION

We describe here a novel protocol for the induction of gonad lineages from human iPSCs with the aim of generating an *in vitro* disease model for DSD. Our protocol uses a stepwise directed differentiation approach to drive iPSCs to bipotential gonad lineages after 7–10 days, followed by the induction of testis cells, in particular, Sertoli-like cells, by days 12–15. This approach allows us

to closely follow the iPSCs as they differentiate through the PS, IM/LPM, bipotential gonad, and early testicular lineages, something not evident in earlier Sertoli cell induction protocols (Bucay et al., 2009; Rodríguez Gutiérrez et al., 2018; Shlush et al., 2017). Furthermore, as our protocol uses growth factor-mediated differentiation, there is no requirement for feeder cells, co-culture, or lentiviral transduction.

Our protocol was adapted from a human kidney differentiation protocol in which iPSCs are induced to traverse through an IM lineage (Takasato et al., 2015). Whereas mouse studies suggest an IM origin for the gonad (Karl and Capel 1998; Sekido and Lovell-Badge 2007), chicken gonad lineage tracing has shown that GPCs arise from the LPM (Yoshino et al., 2016) based on expression of *Foxf1*, which is downregulated in the gonad. The exact origin of the human gonad is not proven. We found that the addition of BMP4 improved bipotential gonad marker expression, with *NR5A1*, *WT1*, and *EMX2* responding to low BMP, while *GADD45g*, *ZFPM2*, *GATA4*, *NR0B1*, and *HSD3B2* were induced with higher BMP4 levels. These data suggest either a more lateral origin for the human bipotential gonad or that two populations of cells contribute, one induced more medially (no or low BMP4, such as the IM) and the other more laterally (higher BMP4, LPM). It should be noted that *WT1* and *EMX2* are also expressed in the fetal kidney, so by patterning for IM (FGF9-only treatment) we may be generating mesonephros, a tissue that is also known to contribute to testis development (Martineau et al., 1997), specifically providing a population of endothelial cells (Combes et al., 2009).

Whereas most bipotential gonad markers were induced by day 10, *NR5A1*, a key gene in bipotential gonad development (Luo et al., 1994), was generally low in monolayer cultures. Unlike most of our other markers, *NR5A1* had reasonable expression in the undifferentiated day 0 iPSCs that we normalized against, somewhat masking the extent of *NR5A1* expression at later stages. This may be confounded by *NR5A1* expression being restricted to a small subset of cells. However, stronger *NR5A1* induction was observed in the 3D gonadal organoid cultures, suggesting that *NR5A1* expression requires a more complex tissue structure or additional factors. Following bipotential gonad differentiation, we see cells committing to a testis-specific fate, with expression of *SOX9* and *AMH*. *In vivo*, these genes are downstream of the master sex-determining gene, *SRY*. Indeed, many bipotential gonad genes, such as *GADD45g*, *GATA4*, or *NR5A1*, upregulate *SRY* (Eggers et al., 2014). Despite expression of many of these bipotential gonad markers, we failed to detect *SRY* RNA expression (data not shown). In the absence of an SRY antibody, we were also unable to assess protein level. Testis development can progress in the absence of *SRY* if *SOX9* is upregulated instead (Huang et al., 1999; Vidal et al., 2001), and we introduce the *SOX9*-activating factor *FGF9* during days 4–7, which may also activate its own expression, as we see a peak of *FGF9* RNA expression at day 7. Subsequently, we see *SOX9* peak between days 7 and 10, followed by an increase in *AMH* between day 10 and day 15. Importantly, *SOX9* expression is observed even in a female iPSC line, where *SRY* is not present. Once *SOX9* is expressed, it maintains its expression via auto-regulation by factors such as PGD_2 (Malki et al., 2005; Wilhelm et al., 2005), which can sex-reverse XX mouse gonads cultured *ex vivo* (Adams and McLaren 2002; Gustin et al., 2016). We found that PGD_2 acts as a positive inducer of the testis pathway and, with extended culture (up to 21 days), differentiated monolayers showed extensive SOX9.

After 14 days of organoid culture, we observed higher expression of the key Sertoli cell markers (*SOX9*, *DHH*, *AMH*, *CLDN11*), indicating that differentiation may be more efficient in a 3D culture. We also saw the emergence of structures/cell clusters expressing Sertoli markers and basement membrane proteins in an "irregular wavy" fashion, as has been described for seminiferous tubules (Dobashi et al., 2003). *In vivo*, Sertoli cells trigger Leydig cell development (Yao et al., 2002) via DHH, which then relies on both the master transcription factor *STAR* and *NR5A1*. Whereas most of our markers indicate we are differentiating Sertoli-like cells, Leydig-like cells may also be arising. Intriguingly, both *DHH* and *NR5A1* were consistently low in monolayer cultures, but showed good induction in 3D culture. At the protein level, a subset of cells (in both monolayer and organoid) express the Leydig marker STAR, although staining was also observed in day 0 iPSCs, and in human scRNA-seq data *STAR* has substantial expression in Sertoli cells (Li et al., 2017), calling into question its specificity. At the RNA level, we observed expression of several Leydig markers by day 21. Taking these results together, we believe that our 3D organoid protocol will enable better interaction between different cell lineages, in the future allowing us to create a more complete human embryonic testis model.

In summary, this work represents a significant advance toward the generation of human embryonic testis tissue from human iPSCs as a disease model. Beyond the DSD field, this system could also benefit germ cell and fertility preservation research. Human germ cells have been successfully differentiated from iPSCs (Yamashiro et al., 2018), and in the future, co-culture of iPSC-derived germ cells with our iPSC-derived testicular cells may help to build a more complete model of the human gonad.

EXPERIMENTAL PROCEDURES

Human Fetal Testis Immunofluorescence

Human fetal testis tissue was obtained following elective termination of pregnancy during the first trimester at the departments of gynecology at Copenhagen University Hospital (Rigshospitalet) and Hvidovre Hospital, Denmark, following informed written and oral consent (ethics permit H-1-2012-007). None of the terminations were for fetal or pregnancy pathology. Fetal age was determined by crown-rump length and foot length (Evtouchenko et al., 1996). Isolated fetal testes were immediately fixed in formalin and embedded in paraffin and sectioned. The sections were de-waxed by two 2-min washes in xylene, followed by an ethanol series (100%, 90%, 80%, 70%, 50%). Antigen retrieval was accomplished by two 5-min washes in 0.1 M citrate buffer in the microwave on high. The sections were blocked with horse serum (10%) for 2 h. Then they were incubated with primary antibodies overnight at 4°C, followed by secondary antibody at room temperature for 2 h. Finally, slides were washed in PBS three times for 5 min (second wash with 1:5000 DAPI) (Thermo Fisher Scientific). Slides were mounted in Fluorsave (Merck) and imaged on a confocal microscope (LSM780, Zeiss). Antibody dilutions are shown in Table S3.

Human iPSC Culture and Monolayer Differentiation

Most differentiation experiments were performed using two feeder-free human iPSC lines: CRL1502 clone C32 (generated by E.J. Wolvetang, The University of Queensland, Australia) (female) and PCS_201_010 iPS clone 5 (American Type Culture Collection, USA) (male). iPSCs were expanded in Essential 8 medium (E8; Thermo Fisher Scientific). One day prior to differentiation, the cells were plated at 10,000 cells/cm^2 on Vitronectin (STEMCELL Technologies) or Matrigel (Corning), as described previously (Takasato et al., 2015, 2016). On day 0 the medium was replaced with Essential 6 medium (E6), either commercial (Thermo Fisher Scientific) or home-made (500 mL DMEM/F12 medium [Thermo Fisher Scientific], 270 mg sodium bicarbonate, 7 μg sodium selenite, 32 mg L-ascorbic acid 2-phosphate sesquimagnesium salt hydrate [Sigma-Aldrich], 5 mg Holo-Transferrin [Sigma-Aldrich], and 10 mg insulin [Sigma-Aldrich]). CHIR (3 μM; R&D Systems) was added for 4 days and then the medium was supplemented with 200 ng/mL FGF9 (R&D Systems), 1 μg/mL heparin (Sigma-Aldrich), and 10 ng/mL BMP4 (R&D Systems) for the next 3 days. Cells were then cultured without any growth factors for 3 days and then treated with 500 ng/mL PGD_2 (Cayman Chemical). Note that throughout all differentiations the medium was changed every 2 days. The following are exceptions to this protocol.

Testing CHIR Duration

On day 0, E8 was replaced with APEL (STEMCELL Technologies, #5210, discontinued) containing CHIR at 4 μM, for 3, 4, and 5 days. The medium was replaced with APEL supplemented with 200 ng/mL FGF9 and 1 μg/mL heparin for a further 4, 3, and 2 days, respectively.

Testing CHIR Concentration

On day 0, E8 was replaced with E6 containing CHIR at 3, 4, or 5 μM for a duration of 4 days and then E6 supplemented with 200 ng/mL FGF9, 1 μg/mL heparin, and 10 ng/mL BMP4 for a further 3 days. Cells were then cultured in E6 with no growth factors for a further 5 days.

Testing BMP4 Concentration

On day 0, E8 was replaced with APEL2 (STEMCELL Technologies, #05275) containing CHIR at 4 μM for 4 days. The medium was then changed to APEL2 supplemented with 200 ng/mL FGF9 and 1 μg/mL heparin, with or without the addition of BMP4 at a concentration of 0, 5, or 50 ng/mL for a further 3 days.

Initial exploratory screens (i.e., CHIR concentration and duration, BMP concentration, SAG and RA treatment) were carried out in one, two, or three independent differentiation experiments, with three technical replicates (separate wells) analyzed statistically. The final monolayer differentiation protocol was carried out four times (i.e., biological replicates) with PCS_201_010, with five biological replicates for CRL1502.3. See figure legends for replicate details.

Organoid Generation

PCS_201_010 iPS clone 5 cells were expanded feeder free in E8. At day −1 cells were plated at 10,000 cells/cm^2 on Vitronectin. On day 0, the medium was replaced with home-made E6 and 3 μM CHIR for 4 days and then E6 + 200 ng/mL FGF9, 1 μg/mL heparin, and 10 ng/mL BMP4 for 3 days. On day 7, the cells were pelleted as described previously (Takasato et al., 2015). Briefly, the cells were dissociated with TrypLE Select (Thermo Fisher Scientific) for 2 min at 37°C. Per organoid, 350,000 cells were pelleted (300 rcf for 3 min, three times, with 180° rotation between spins) and transferred to Transwell filters (Corning) using wide-bore pipette tips (Sigma-Aldrich). The cell pellets were cultured without any growth factors for 3 days, followed by treatment with 500 ng/mL PGD_2 supplement. The medium was changed every 2 days.

Gene Expression Analysis

RNA was extracted using TRIzol reagent (Thermo Fisher) or the ReliaPrep RNA Cell Miniprep System (Promega), followed by DNase treatment (Promega). cDNA was synthesized using the GoScript reverse transcriptase system (Promega). qRT-PCR was performed with GoTaq qPCR Master Mix (Promega) on the LightCycler480 (Roche) with *GAPDH* as the reference gene. qPCR technical duplicates were used for each technical replicate. Data were normalized to *GAPDH* and then normalized to control d0 samples (ΔΔCt method). Primer sequences can be found in Table S2.

SUPPLEMENTAL INFORMATION

Supplemental Information can be found online at https://doi.org/10.1016/j.stemcr.2020.10.009.

AUTHOR CONTRIBUTIONS

Conceptualization, I.M.K., S.P., M.T., M.H.L., A.H.S., and K.L.A.; Methodology, I.M.K., S.P., M.H.L., A.H.S., and K.L.A.; Investigation, I.M.K., S.P., E.G., G.R., K.L.A., M.T., and P.X.E.; Formal Analysis, I.M.K. and S.P.; Validation, I.M.K. and S.P.; Resources, I.G., A.N.C., and A.J.; Writing – Original Draft, I.M.K., K.L.A., S.P., M.H.L., A.N.C., and A.H.S.; Writing – Review & Editing, I.M.K., K.L.A., S.P., G.R., M.H.L., A.N.C., A.J., and A.H.S.; Visualization, I.M.K., S.P., and K.L.A.; Supervision, K.L.A., M.H.L., A.N.C., and

A.H.S.; Project Administration, K.L.A. and S.P.; Funding Acquisition, K.L.A., I.M.K., S.P., and A.H.S.

ACKNOWLEDGMENTS

This project was funded by an NHMRC Ideas grant (K.L.A., APP1156942) and Program grant (A.H.S., APP1074258) from the National Health and Medical Research Council (NHMRC), Australia. I.M.K was funded by a Research Training Scheme scholarship, The University of Melbourne, and an International Foundation for Ethical Research (IFER) graduate fellowship. M.H.L. and A.H.S. are Senior Principal Research Fellows of the NHMRC, Australia (APP1136085 and APP1154187 respectively).

Received: April 17, 2020
Revised: October 21, 2020
Accepted: October 21, 2020
Published: November 19, 2020

REFERENCES

Adams, I.R., and McLaren, A. (2002). Sexually dimorphic development of mouse primordial germ cells: switching from oogenesis to spermatogenesis. Development *129*, 1155–1164.

Belle, M., Godefroy, D., Couly, G., Malone, S.A., Collier, F., Giacobini, P., and Chédotal, A. (2017). Tridimensional Visualization and analysis of early human development. Cell *169*, 161–173.e12.

Bowles, J., Knight, D., Smith, C., Wilhelm, D., Richman, J., Mamiya, S., Yashiro, K., Chawengsaksophak, K., Wilson, M.J., Rossant, J., et al. (2006). Retinoid signaling determines germ cell fate in mice. Science *312*, 596–600.

Bucay, N., Yebra, M., Cirulli, V., Afrikanova, I., Kaido, T., Hayek, A., and Montgomery, A.M.P. (2009). A novel approach for the derivation of putative primordial germ cells and sertoli cells from human embryonic stem cells. Stem Cells *27*, 68–77.

Buganim, Y., Itskovich, E., Hu, Y.-C., Cheng, A.W., Ganz, K., Sarkar, S., Fu, D., Welstead, G.G., Page, D.C., and Jaenisch, R. (2012). Direct reprogramming of fibroblasts into embryonic Sertoli-like cells by defined factors. Cell Stem Cell *11*, 373–386.

Chen, X., Li, C., Chen, Y., Xi, H., Zhao, S., Ma, L., Xu, Z., Han, Z., Zhao, J., Ge, R., et al. (2019). Differentiation of human induced pluripotent stem cells into Leydig-like cells with molecular compounds. Cell Death Dis. *10*, 220.

Combes, A.N., Phipson, B., Lawlor, K.T., Dorison, A., Patrick, R., Zappia, L., Harvey, R.P., Oshlack, A., and Little, M.H. (2019). Single cell analysis of the developing mouse kidney provides deeper insight into marker gene expression and ligand-receptor crosstalk. Development *146*, dev178673.

Combes, A.N., Wilhelm, D., Davidson, T., Dejana, E., Harley, V., Sinclair, A., and Koopman, P. (2009). Endothelial cell migration directs testis cord formation. Dev. Biol. *326*, 112–120.

Darde, T.A., Lecluze, E., Lardenois, A., Stévant, I., Alary, N., Tüttelmann, F., Collin, O., Nef, S., Jégou, B., Rolland, A.D., et al. (2019). The ReproGenomics Viewer: a multi-omics and cross-species resource compatible with single-cell studies for the reproductive science community. Bioinformatics *35*, 3133–3139.

Darde, T.A., Sallou, O., Becker, E., Evrard, B., Monjeaud, C., Le Bras, Y., Jégou, B., Collin, O., Rolland, A.D., and Chalmel, F. (2015). The ReproGenomics Viewer: an integrative cross-species toolbox for the reproductive science community. Nucleic Acids Res. *43*, W109–W116.

Del Valle, I., Buonocore, F., Duncan, A.J., Lin, L., Barenco, M., Parnaik, R., Shah, S., Hubank, M., Gerrelli, D., and Achermann, J.C. (2017). A genomic atlas of human adrenal and gonad development. Wellcome Open Res. *2*, 25.

Dobashi, M., Fujisawa, M., Naito, I., Yamazaki, T., Okada, H., and Kamidono, S. (2003). Distribution of type IV collagen subtypes in human testes and their association with spermatogenesis. Fertil. Steril *80*, 755–760.

Duester, G. (2008). Retinoic acid synthesis and signaling during early organogenesis. Cell *134*, 921–931.

Eggers, S., Ohnesorg, T., and Sinclair, A. (2014). Genetic regulation of mammalian gonad development. Nat. Rev. Endocrinol. *10*, 673–683.

Eggers, S., Sadedin, S., van den Bergen, J.A., Robevska, G., Ohnesorg, T., Hewitt, J., Lambeth, L., Bouty, A., Knarston, I.M., Tan, T.Y., et al. (2016). Disorders of sex development: insights from targeted gene sequencing of a large international patient cohort. Genome Biol. *17*, 243.

Escalante-Alcalde, D., and Merchant-Larios, H. (1992). Somatic and germ cell interactions during histogenetic aggregation of mouse fetal testes. Exp. Cell Res. *198*, 150–158.

Evtouchenko, L., Studer, L., Spenger, C., Dreher, E., and Seiler, R.W. (1996). A mathematical model for the estimation of human embryonic and fetal age. Cell Transpl. *5*, 453–464.

Gell, J.J., Liu, W., Sosa, E., Chialastri, A., Hancock, G., Tao, Y., Wamaitha, S.E., Bower, G., Dey, S.S., and Clark, A.T. (2020). An extended culture system that supports human primordial germ cell-like cell survival and initiation of DNA methylation erasure. Stem Cell Rep. *14*, 1–14.

Guo, F., Yan, L., Guo, H., Li, L., Hu, B., Zhao, Y., Yong, J., Hu, Y., Wang, X., Wei, Y., et al. (2015). The transcriptome and DNA methylome landscapes of human primordial germ cells. Cell *161*, 1437–1452.

Gustin, S., Stringer, J., Hogg, K., Sinclair, A., and Western, P. (2016). FGF9, Activin and TGFβ promote testicular characteristics in an XX gonad organ culture model. Reprod. Rep. *16*, 0293.

Hayashi, K., Ohta, H., Kurimoto, K., Aramaki, S., and Saitou, M. (2011). Reconstitution of the mouse germ cell specification pathway in culture by pluripotent stem cells. Cell *146*, 519–532.

Hikabe, O., Hamazaki, N., Nagamatsu, G., Obata, Y., Hirao, Y., Hamada, N., Shimamoto, S., Imamura, T., Nakashima, K., Saitou, M., and Hayashi, K. (2016). Reconstitution in vitro of the entire cycle of the mouse female germ line. Nature *539*, 299–303.

Huang, B., Wang, S., Ning, Y., Lamb, A.N., and Bartley, J. (1999). Autosomal XX sex reversal caused by duplication of SOX9. Am. J. Med. Genet. *87*, 349–353.

Hughes, I.A., Houk, C., Ahmed, S.F., and Lee, P.A.; Lawson Wilkins Pediatric Endocrine Society/European Society for Paediatric Endocrinology Consensus Group (2006). Consensus statement on management of intersex disorders. J. Pediatr. Urol. *2*, 148–162.

Irie, N., Weinberger, N., Tang, W., Kobayashi, T., Viukov, S., Manor, Y.S., Dietmann, S., Hanna, J., and Surani, M.A. (2015). SOX17 is a critical specifier of human primordial germ cell fate. Cell *160*, 253–268.

Jadhav, U., and Jameson, J.L. (2011). Steroidogenic factor-1 (SF-1)-driven differentiation of murine embryonic stem (ES) cells into a gonadal lineage. Endocrinology *152*, 2870–2882.

Karl, J., and Capel, B. (1998). Sertoli cells of the mouse testis originate from the coelomic epithelium. Dev. Biol. *203*, 323–333.

Kjartansdóttir, K.R., Reda, A., Panula, S., Day, K., Hultenby, K., Soder, O., Hovatta, O., and Stukenborg, J.-B. (2015). A combination of culture conditions and gene expression analysis can Be used to investigate and predict hES cell differentiation potential towards male gonadal cells. PLoS One *10*, e0144029.

Lancaster, M.A., and Knoblich, J.A. (2014). Generation of cerebral organoids from human pluripotent stem cells. Nat. Protoc. *9*, 2329–2340.

Li, L., Dong, J., Yan, L., Yong, J., Liu, X., Hu, Y., Fan, X., Wu, X., Guo, H., Wang, X., et al. (2017). Single-cell RNA-seq analysis maps development of human germline cells and gonadal Niche interactions. Cell Stem Cell *20*, 858–873.

Liang, J., Wang, N., He, J., Du, J., Guo, Y., Li, L., Wu, W., Yao, C., Li, Z., and Kee, K. (2019). Induction of Sertoli-like cells from human fibroblasts by NR5A1 and GATA4. Elife *8*, 301.

Lindström, N.O., McMahon, J.A., Guo, J., Tran, T., Guo, Q., Rutledge, E., Parvez, R.K., Saribekyan, G., Schuler, R.E., Liao, C., et al. (2018). Conserved and divergent features of human and mouse kidney organogenesis. J. Am. Soc. Nephrol. *29*, 785–805.

Luo, X.R., Ikeda, Y.Y., and Parker, K.L. (1994). A cell-specific nuclear receptor is essential for adrenal and gonadal development and sexual differentiation. Cell *77*, 481–490.

Malki, S., Nef, S., Notarnicola, C., Thevenet, L., Gasca, S., Mejean, C., Berta, P., Poulat, F., and Boizet-Bonhoure, B. (2005). Prostaglandin D2 induces nuclear import of the sex-determining factor SOX9 via its cAMP-PKA phosphorylation. EMBO J. *24*, 1798–1809.

Martineau, J., Nordqvist, K., Tilmann, C., Lovell-Badge, R., and Capel, B. (1997). Male-specific cell migration into the developing gonad. Curr. Biol. *7*, 958–968.

McCracken, K.W., Howell, J.C., Wells, J.M., and Spence, J.R. (2011). Generating human intestinal tissue from pluripotent stem cells in vitro. Nat. Protoc. *6*, 1920–1928.

McLaren, A., and Southee, D. (1997). Entry of mouse embryonic germ cells into meiosis. Dev. Biol. *187*, 107–113.

Phipson, B., Er, P.X., Combes, A.N., Forbes, T.A., Howden, S.E., Zappia, L., Yen, H.-J., Lawlor, K.T., Hale, L.J., Sun, J., et al. (2019). Evaluation of variability in human kidney organoids. Nat. Meth. *16*, 79–87.

Rodríguez Gutiérrez, D., Eid, W., and Biason-Lauber, A. (2018). A human gonadal cell model from induced pluripotent stem cells. Front. Genet. *9*, 498.

Sandell, L.L., Sanderson, B.W., Moiseyev, G., Johnson, T., Mushegian, A., Young, K., Rey, J.-P., Ma, J.-X., Staehling-Hampton, K., and Trainor, P.A. (2007). RDH10 is essential for synthesis of embryonic retinoic acid and is required for limb, craniofacial, and organ development. Genes Dev. *21*, 1113–1124.

Satoh, M. (1991). Histogenesis and organogenesis of the gonad in human embryos. J. Anat. *177*, 85–107.

Sekido, R., and Lovell-Badge, R. (2007). Mechanisms of gonadal morphogenesis are not conserved between chick and mouse. Dev. Biol. *302*, 132–142.

Sepponen, K., Lundin, K., Knuus, K., Väyrynen, P., Raivio, T., Tapanainen, J.S., and Tuuri, T. (2017). The role of sequential BMP signaling in directing human embryonic stem cells to bipotential gonadal cells. J. Clin. Endocrinol. Metab. *102*, 4303–4314.

Shlush, E., Maghen, L., Swanson, S., Kenigsberg, S., Moskovtsev, S., Barretto, T., Gauthier-Fisher, A., and Librach, C.L. (2017). In vitro generation of Sertoli-like and haploid spermatid-like cells from human umbilical cord perivascular cells. Stem Cell Res. Ther. *8*, 37.

Stévant, I., Kuhne, F., Greenfield, A., Chaboissier, M.-C., Dermitzakis, E.T., and Nef, S. (2019). Dissecting cell lineage specification and sex fate determination in gonadal somatic cells using single-cell transcriptomics. Cell Rep. *26*, 3272–3283.

Takasato, M., Er, P.X., Becroft, M., Vanslambrouck, J.M., Stanley, E.G., Elefanty, A.G., and Little, M.H. (2014). Directing human embryonic stem cell differentiation towards a renal lineage generates a self-organizing kidney. Nat. Cell Biol. *16*, 118–126.

Takasato, M., Er, P.X., Chiu, H.S., and Little, M.H. (2016). Generation of kidney organoids from human pluripotent stem cells. Nat. Protoc. *11*, 1681–1692.

Takasato, M., Er, P.X., Chiu, H.S., Maier, B., Baillie, G.J., Ferguson, C., Parton, R.G., Wolvetang, E.J., Roost, M.S., Chuva de Sousa Lopes, S.M., et al. (2015). Kidney organoids from human iPS cells contain multiple lineages and model human nephrogenesis. Nature *526*, 564–568.

Takasato, M., and Little, M.H. (2015). The origin of the mammalian kidney: implications for recreating the kidney in vitro. Development *142*, 1937–1947.

Vidal, V.P., Chaboissier, M.C., de Rooij, D.G., and Schedl, A. (2001). Sox9 induces testis development in XX transgenic mice. Nat. Genet. *28*, 216–217.

Wilhelm, D., Martinson, F., Bradford, S., Wilson, M.J., Combes, A.N., Beverdam, A., Bowles, J., Mizusaki, H., and Koopman, P. (2005). Sertoli cell differentiation is induced both cell-autonomously and through prostaglandin signaling during mammalian sex determination. Dev. Biol. *287*, 111–124.

Yamashiro, C., Sasaki, K., Yabuta, Y., Kojima, Y., Nakamura, T., Okamoto, I., Yokobayashi, S., Murase, Y., Ishikura, Y., Shirane, K., et al. (2018). Generation of human oogonia from induced pluripotent stem cells in vitro. Science *362*, 356–360.

Yang, L., Soonpaa, M.H., Adler, E.D., Roepke, T.K., Kattman, S.J., Kennedy, M., Henckaerts, E., Bonham, K., Abbott, G.W., Linden, R.M., et al. (2008). Human cardiovascular progenitor cells develop from a KDR+ embryonic-stem-cell-derived population. Nature *453*, 524–528.

Yang, Y., Li, Z., Wu, X., Chen, H., Xu, W., Xiang, Q., Zhang, Q., Chen, J., Ge, R.-S., Su, Z., et al. (2017). Direct reprogramming of mouse fibroblasts toward leydig-like cells by defined factors. Stem Cell Rep. *8*, 39–53.

Yang, Y., Su, Z., Xu, W., Luo, J., Liang, R., Xiang, Q., Zhang, Q., Ge, R.-S., and Huang, Y. (2015). Directed mouse embryonic stem cells

into leydig-like cells rescue testosterone-deficient male rats in vivo. Stem Cells Dev. *24*, 459–470.

Yao, H.H., Whoriskey, W., and Capel, B. (2002). Desert Hedgehog/Patched 1 signaling specifies fetal Leydig cell fate in testis organogenesis. Genes Dev. *16*, 1433–1440.

Yazawa, T., Mizutani, T., Yamada, K., Kawata, H., Sekiguchi, T., Yoshino, M., Kajitani, T., Shou, Z., Umezawa, A., and Miyamoto, K. (2006). Differentiation of adult stem cells derived from bone marrow stroma into Leydig or adrenocortical cells. Endocrinology *147*, 4104–4111.

Yoshino, T., Murai, H., and Saito, D. (2016). Hedgehog-BMP signalling establishes dorsoventral patterning in lateral plate mesoderm to trigger gonadogenesis in chicken embryos. Nat. Commun. *7*, 12561.

Zhao, L., Wang, C., Lehman, M.L., He, M., An, J., Svingen, T., Spiller, C.M., Ng, E.T., Nelson, C.C., and Koopman, P. (2018). Transcriptomic analysis of mRNA expression and alternative splicing during mouse sex determination. Mol. Cell Endocrinol. *478*, 84–96.